

Fermi National Accelerator Laboratory

FERMILAB-Conf-92/274

The DØ Experiment at Fermilab

Ulrich Heintz

*Columbia University
Nevis Laboratories
P.O. Box 137, Irvington, NY 10533
for the DØ Collaboration
Fermi National Accelerator Laboratory
P.O. Box 500, Batavia, Illinois 60510*

October 1992

Presented at the *4th Topical Seminar on "The Standard Model and just Beyond"*
San Miniato, Italy, June 1-5, 1992



Disclaimer

This report was prepared as an account of work sponsored by an agency of the United States Government. Neither the United States Government nor any agency thereof, nor any of their employees, makes any warranty, express or implied, or assumes any legal liability or responsibility for the accuracy, completeness, or usefulness of any information, apparatus, product, or process disclosed, or represents that its use would not infringe privately owned rights. Reference herein to any specific commercial product, process, or service by trade name, trademark, manufacturer, or otherwise, does not necessarily constitute or imply its endorsement, recommendation, or favoring by the United States Government or any agency thereof. The views and opinions of authors expressed herein do not necessarily state or reflect those of the United States Government or any agency thereof.

THE DØ EXPERIMENT AT FERMILAB

ULRICH HEINTZ

*Nevis Laboratories, Columbia University, P.O. Box 137
Irvington, NY 10533, U.S.A.*for the
DØ COLLABORATION*

ABSTRACT

The DØ experiment at Fermilab is described. The detector is complete and presently taking physics data. Results from beam tests of the calorimeter and an outline of the physics agenda for the present run are also given.

1. The DØ Detector

1.1. Detector Design

The DØ detector¹ has been designed as a detector for high p_T physics in $\bar{p}p$ interactions at a center of mass energy around 2 TeV. The decision was taken not to have a central magnetic field. Instead, the design put emphasis on excellent lepton detection capabilities. The detector has a very uniform and hermetic calorimeter coverage over a large range in pseudorapidity (η) and muon coverage over 98% of the solid angle. The calorimeter provides good energy resolution for electromagnetic and hadronic showers and through its hermiticity good missing E_T resolution.

Figure 1 shows a cut out picture of the entire detector. Located immediately around the beam pipe are the tracking chambers. They are surrounded by the central calorimeter and the two end calorimeters. The muon toroids and chambers of the muon detection system surround the entire detector. In the following I will

* The DØ collaboration: Universidad de los Andes, Bogota, Colombia; University of Arizona; Brookhaven National Laboratory; Brown University; University of California, Riverside; Centro Brasileiro de Pesquisas Fisicas, Rio de Janeiro, Brasil; CINVESTAV, Mexico City, Mexico; Columbia University; Delhi University, Delhi, India; Fermi National Accelerator Laboratory; Florida State University; University of Hawaii; University of Illinois, Chicago; Indiana University; Iowa State University; Lawrence Berkeley Laboratory; University of Maryland; University of Michigan; Michigan State University; Moscow State University, Russia; New York University; Northeastern University; Northern Illinois University; Northwestern University; University of Notre Dame; Panjab University, Chandigarh, India; Institute for High Energy Physics, Protvino, Russia; Purdue University; Rice University; University of Rochester; CEN Saclay, France; State University of New York, Stony Brook; Superconducting Supercollider Laboratory, Dallas; Tata Institute of Fundamental Research, Bombay, India; University of Texas, Arlington; Texas A&M University

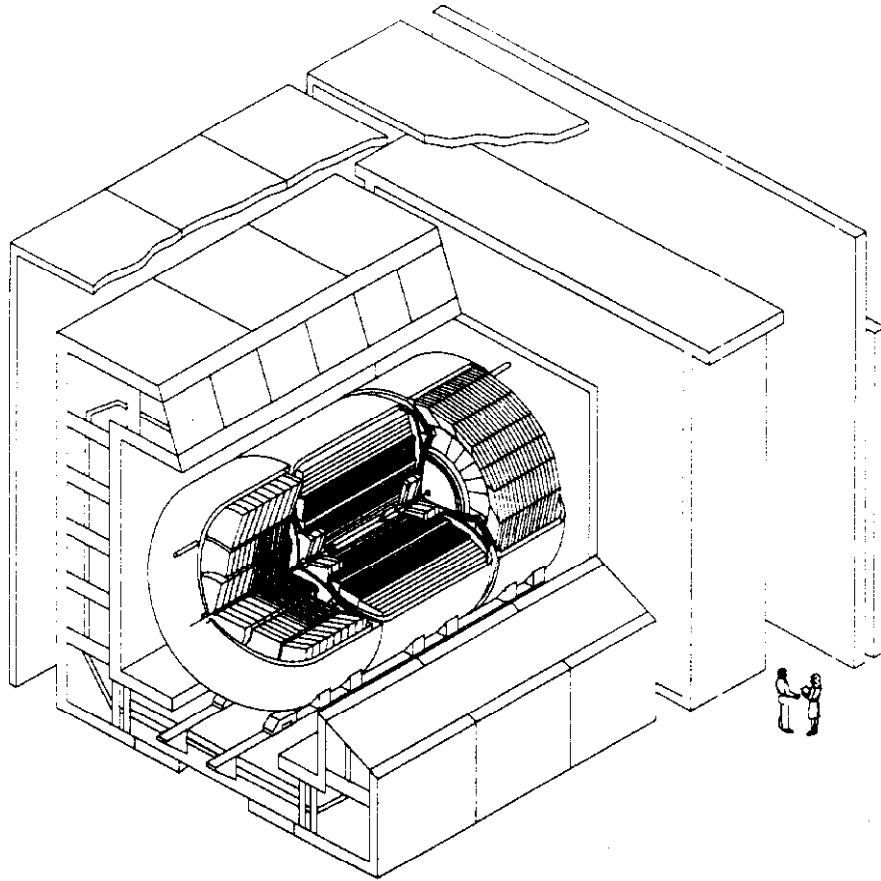


Fig. 1. The DØ detector.

describe the parts of the detector in some more detail.

1.2. Central Tracking System

The central tracking system consists of four subdetectors. Innermost is the vertex chamber, a jet type drift chamber. It has three layers with eight sense wires each. Its resolution in drift direction is $30\text{--}80\ \mu\text{m}$. The coordinate along the beam direction is measured using charge division on the sense wires and cathode pads. The resolution in this direction is $4\text{--}10\ \text{mm}$.

The next outer subdetector is the transition radiation detector, also consisting of three layers. Test beam results show that it is capable of a 50:1 electron to pion rejection at 90% electron efficiency.

The central drift chamber is located directly in front of the central calorimeter. It has four layers with seven sense wires each. Its resolution in drift direction is less than $200\ \mu\text{m}$. The position of tracks in the z direction is measured using delay lines. There are two delay lines in every cell which couple to the two outermost

sense wires. They achieve a resolution of 4 mm along their length. The central drift chamber covers the pseudorapidity region $|\eta| < 1$.

The forward and backward directions are covered by the forward drift chambers. They consist of one ϕ -chamber and two θ -chambers. The θ -chambers are each six sense wires deep with the sense wires oriented transversely to the beam. The ϕ chamber is eight sense wires deep with the sense wires oriented radially outward from the beam. The resolution is typically 200 μm .

1.3. Calorimeter

The modules of the uranium-liquid argon sampling calorimeter are located in three cryostats (figure 2). In every cryostat there are three different sections. Innermost is the electromagnetic (EM) section. With 3 mm uranium plates it has the finest sampling. The EM section is read out in four layers, 2, 2, 7, and 10 radiation lengths (X_0) thick for a total thickness of 21 X_0 . The fractional energy resolution has been measured to be $16\%/\sqrt{E}$.

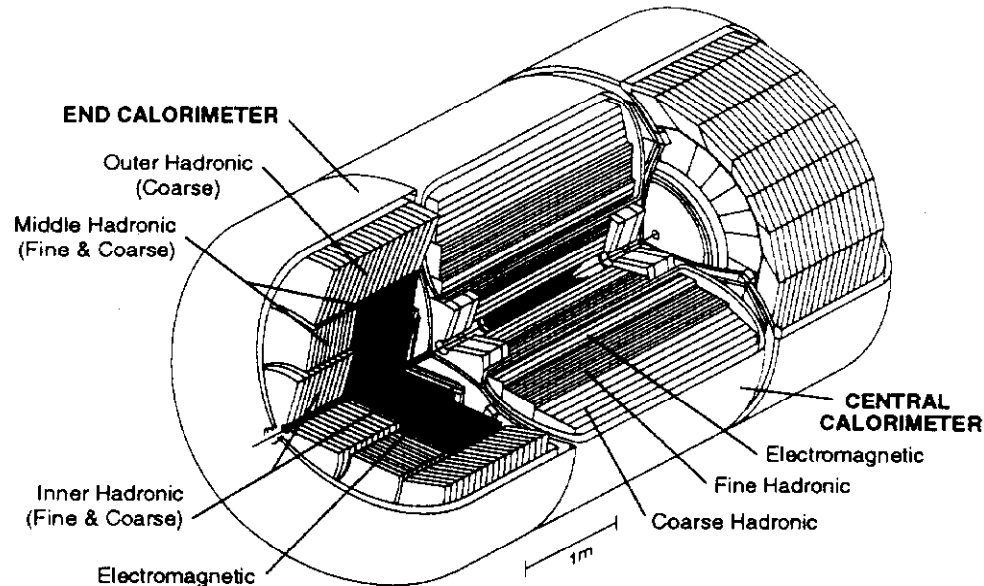


Fig. 2. The DØ calorimeter.

Behind the EM section is the fine hadronic section (FH) with somewhat coarser sampling. It consists of 6 mm uranium plates and is read out in three or four longitudinal segments. The energy resolution of the FH calorimeter is $50\%/\sqrt{E}$. The coarse hadronic (CH) section consists of 46.5mm thick copper or steel plates and serves as a leakage detector.

All modules are subdivided into pseudoprojective towers. The transverse segmentation is very fine, $\Delta\eta \times \Delta\phi = 0.1 \times 0.1$, except for the third EM layer in

which it is $\Delta\eta \times \Delta\phi = 0.05 \times 0.05$.

1.4. Muon System

The muon system consists of five steel toroids 1.1–1.5 meters thick. The central toroid surrounds the calorimeter and covers the region $50^\circ < \theta < 135^\circ$ in colatitude θ . The end toroids and the small angle muon system cover the forward regions down to 3° from the beam, resulting in a muon coverage for $|\eta| < 3$. Tracking of muons is accomplished by three layers of proportional drift tubes. The innermost layer is located between calorimeter and steel. Together with the central tracking it provides a measurement of the initial direction of the muon. The other two layers are located outside the steel. They measure the direction in which the muon exits the steel. The chambers are oriented so that the drift direction is in bend direction of the magnet. From the change of direction of the particle in the magnetized steel toroids we measure its momentum. Up to momenta of 50–100 GeV the resolution is limited by multiple scattering in calorimeter and toroids to $\Delta p/p \approx 20\%$. There are 13–19 absorption lengths of material between interaction point and the outer two muon chambers. Therefore the probability for pion punch-through is small.

2. Beam Test Results

Extensive beam tests of the calorimeter modules have been performed. The goals of these tests were to obtain an absolute calibration of the energy scale, to measure energy resolution and shower shapes. The test beam delivered the data necessary to develop a simulation which models the response of the detector well.

We developed a Monte Carlo simulation that uses GEANT 3.14 to simulate the detector response. It uses EGS4 to simulate electromagnetic showers and GHEISHA for hadrons. For the test beam simulation the complete detector geometry, including every absorber plate and argon gap, was included in the Monte Carlo. With this simulation we achieve excellent agreement with the data.

Detailed energy scans using both electron and pion beams have been performed for both end calorimeter (EC) and central calorimeter (CC) modules. The results quoted here are from the tests of the EC modules². The linearity of the response was measured. In Figure 3(a) we see the fractional deviation of the measured energy of electrons in the calorimeter from their momentum as a function of beam momentum. The electron momentum was measured in wire chambers in front of the calorimeter modules. The response is linear to 0.3% down to 10 GeV beam momentum. In Figure 3(b) the fractional energy resolution for electrons is plotted as a function of beam momentum. It is measured to be $\sigma/E = 0.003 + 0.16\sqrt{\text{GeV}}/\sqrt{E} + 0.3\text{GeV}/E$. Both results are reproduced well by the Monte Carlo simulation. The ratio of electron and pion response was measured to be about 1.05.

The transverse shower profile can be measured by scanning the beam across a calorimeter cell and measuring the fraction of energy deposited outside the cell as

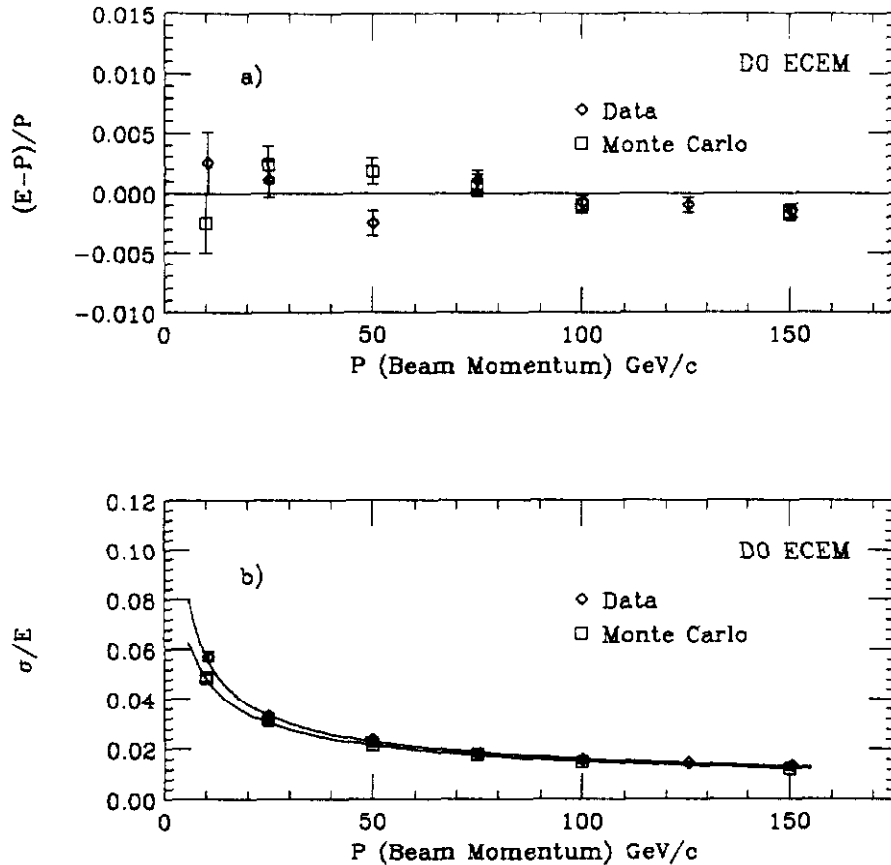


Fig. 3. (a) Linearity of response and (b) energy resolution of the EC-EM calorimeter for electrons.

a function of distance X of the beam from the cell edge. This quantity is plotted in figure 4. Again we achieve excellent agreement between data and Monte Carlo.

3. Collider Operation

The present run, also called run Ia, will continue until the end of March, 1993. The goal for the accelerator is to deliver an integrated luminosity of 25 pb^{-1} . This run will be followed by a four month long shutdown and run Ib, which will last from August, 1993 until May, 1994. We anticipate a total integrated luminosity of about 100 pb^{-1} from runs Ia and Ib.

Until the beginning of September 1992 the Tevatron had delivered an integrated luminosity of 600 nb^{-1} . The luminosity at the beginning of stores is now typically above $10^{30} \text{ cm}^{-2}\text{s}^{-1}$ and is expected to reach $5 \times 10^{30} \text{ cm}^{-2}\text{s}^{-1}$ soon. The DØ detector was completed earlier this year and has been taking data since the beginning of the run. The first $\bar{p}p$ collisions were observed in the DØ detector on May

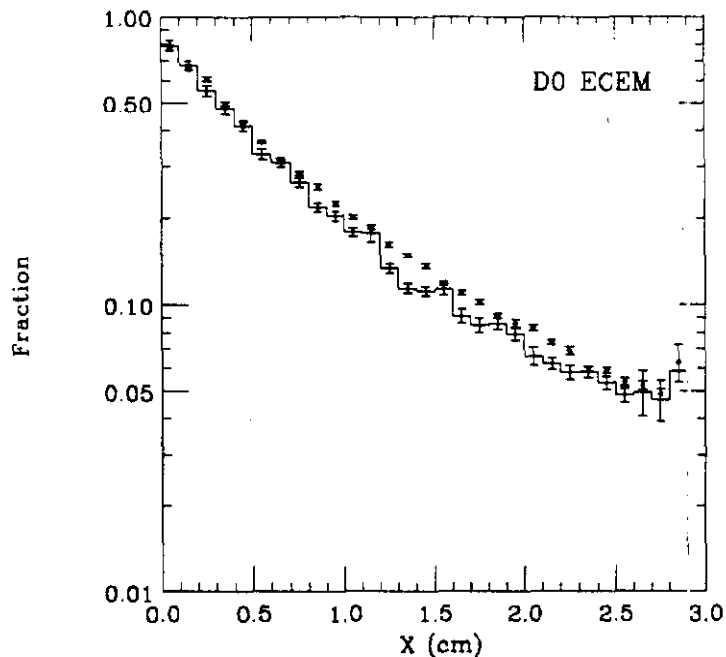


Fig. 4. Transverse profile for 50 GeV electron showers in the EC-EM for data (points) and Monte Carlo (histogram with errors).

12, 1992, two weeks before this presentation was given. The detector has generally been working as expected and we have recorded 150 nb^{-1} of physics data on tape.

Figure 5 shows one of our first $W \rightarrow e\nu$ event candidates. Shown is a side view of the calorimeter and the central tracking system. Calorimeter energies above 1 GeV are summed over the top and bottom halves of the calorimeter and displayed in a greyscale. The cluster of energy deposits in the lower half of the central calorimeter is the electron candidate in this otherwise characteristically quiet event.

4. Physics Agenda

Apart from the search for the top quark and a precision measurement of the mass of the W boson we also expect to make significant contributions to QCD and b -quark physics and search for new phenomena.

If, as the CDF mass limit of 91 GeV^3 implies, the top quark is heavier than the W boson, top quark production at Tevatron energies will be dominated by the process $\bar{p}p \rightarrow t\bar{t} + X$. The top quark will predominantly decay to a W boson and a b quark. Depending on the decay of the W boson we therefore have decay channels with up to two leptons in the final state, accompanied by a number of jets.

The most promising discovery channels are the channels with high p_T elec-

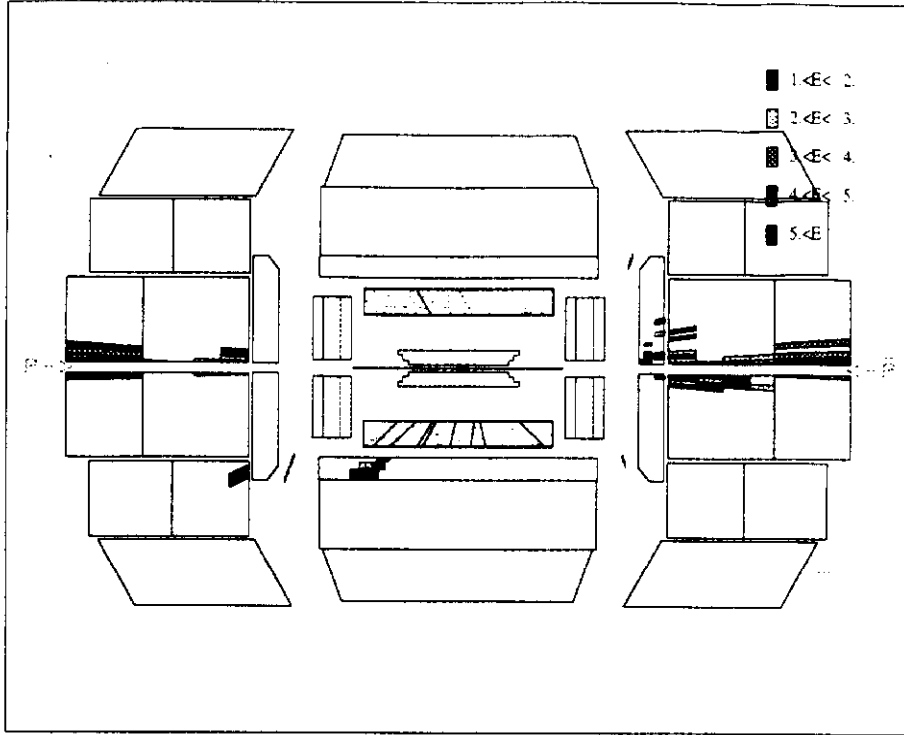


Fig. 5. $W \rightarrow e + \nu$ event candidate.

trons or muons in the final state, $t\bar{t} \rightarrow \ell + \text{jets}$ ($\ell = e$ or μ) with a branching ratio of about 30%, and $t\bar{t} \rightarrow \ell^+\ell^- + \text{jets}$ (5%). Especially the $e\mu$ channel is promising due to its negligible background. If we do not observe any $e\mu$ events in run Ia (25 pb^{-1}) we would be able to put a lower limit on the top quark mass of 140 GeV at 90% confidence level, assuming a detector efficiency \times acceptance of 50%. After run Ib (100 pb^{-1}) the limit would be 175 GeV.

The measurement of the W mass is currently still limited by the number of detected events. With larger event samples not only the statistical error will decrease but also many sources of systematic errors. With the data sample from run Ia and Ib, we hope to measure the W mass to about 120 MeV.

Simultaneous measurements of the masses of the top quark and the W boson will test the standard model and, assuming validity of the standard model, will constrain the mass of the Higgs. Figure 6 shows the mass of the W boson in the standard model as a function of the top mass for Higgs masses of 50, 100, and 1000 GeV. In this figure the LEP measurement of the Z mass of 91.175 GeV⁴ was used. The inset box shows the UA2 and CDF measurements⁵ of the W mass. The horizontal lines show the range of the W mass allowed at the 95% confidence level by a measurement of the W mass with an error of 120 MeV, centered at the combined CDF and UA2 measurement. For Higgs masses below 1 TeV such a measurement would give an upper limit on the mass of a standard model top quark below 200

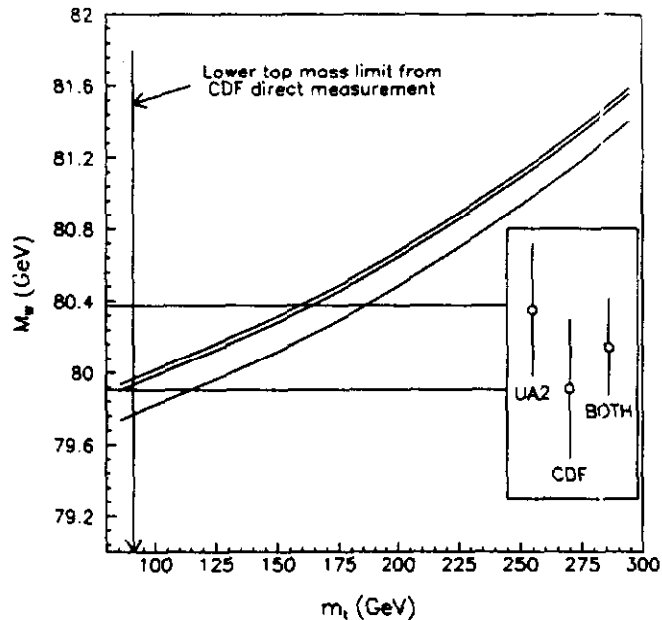


Fig. 6. Standard model dependence of W boson mass M_W on top quark mass m_t for Higgs masses of 50 GeV (top curve), 100 GeV (middle), and 1000 GeV (bottom).

GeV, within the range of discovery at Fermilab.

5. Acknowledgements

I would like to thank my $D\bar{O}$ colleagues for their help in preparing this paper. This work is supported in part by the US National Science Foundation.

6. References

1. $D\bar{O}$ Design Report, 1984 (unpublished)
2. H. Aihara et al., $D\bar{O}$ internal note 1448, accepted for publication by *Nuclear Instruments and Methods in Physics Research* (1992).
3. F. Abe et al. (CDF), FERMILAB-PUB-91-352-E, (1991).
4. W. Hollik, G. Burgers, "Z⁰ Physics at LEP" V1, CERN 89.08 (1989).
5. J. Alitti et al. (UA2), *Phys. Lett.* **B276** (1992) 354; F. Abe et al. (CDF), *Phys. Rev.* **D43** (1991) 2070.